Biogeosciences, 7, 1401–1412, 2010
www.biogeosciences.net/7/1401/2010/
doi:10.5194/bg-7-1401-2010

Biogeosciences

Individual and interacting effects of pCO_2 and temperature on *Emiliania huxleyi* calcification: study of the calcite production, the coccolith morphology and the coccosphere size

C. De Bodt[1], **N. Van Oostende**[2], **J. Harlay**[1,*], **K. Sabbe**[2], **and L. Chou**[1]

[1]Laboratoire d'Océanographie Chimique et Géochimie des Eaux, Université Libre de Bruxelles (ULB), Bruxelles, Belgium
[2]Protistology & Aquatic Ecology, Gent University (UGent), Gent, Belgium
[*]now at: AGO, Unité d'Océanographie Chimique, Université de Liège (ULg), Liège, Belgium

Received: 4 November 2009 – Published in Biogeosciences Discuss.: 27 November 2009
Revised: 8 April 2010 – Accepted: 19 April 2010 – Published: 5 May 2010

Abstract. The impact of ocean acidification and increased water temperature on marine ecosystems, in particular those involving calcifying organisms, has been gradually recognised. We examined the individual and combined effects of increased pCO_2 (180 ppmV CO_2, 380 ppmV CO_2 and 750 ppmV CO_2 corresponding to past, present and future CO_2 conditions, respectively) and temperature (13 °C and 18 °C) during the exponential growth phase of the coccolithophore *E. huxleyi* using batch culture experiments. We showed that cellular production rate of Particulate Organic Carbon (POC) increased from the present to the future CO_2 treatments at 13 °C. A significant effect of pCO_2 and of temperature on calcification was found, manifesting itself in a lower cellular production rate of Particulate Inorganic Carbon (PIC) as well as a lower PIC:POC ratio at future CO_2 levels and at 18 °C. Coccosphere-sized particles showed a size reduction with both increasing temperature and CO_2 concentration. The influence of the different treatments on coccolith morphology was studied by categorizing SEM coccolith micrographs. The number of well-formed coccoliths decreased with increasing pCO_2 while temperature did not have a significant impact on coccolith morphology. No interacting effects of pCO_2 and temperature were observed on calcite production, coccolith morphology or on coccosphere size. Finally, our results suggest that ocean acidification might have a larger adverse impact on coccolithophorid calcification than surface water warming.

Correspondence to: C. De Bodt
(cdebodt@ulb.ac.be)

1 Introduction

The global atmospheric carbon dioxide (CO_2) concentration has increased from a pre-industrial value of about 280 ppmV to 379 ppmV in 2005 (IPCC, 2007). The anthropogenic gas emissions have led to a rise by 0.74±0.18 °C in global average surface temperature from 1906 to 2005 (IPCC, 2007). One fourth of the CO_2 emitted to the atmosphere is absorbed by the ocean (Canadell et al., 2007) where CO_2 dissolves in the surface waters, decreasing the seawater pH, the availability of carbonate ions, and the saturation state of seawater with respect to calcium carbonates (Zeebe and Wolf-Gladrow, 2001). Global warming results in an enhancement in vertical stratification of the water column, leading therefore to a decreased mixing between the surface ocean and the deeper layers with a consequent decrease in the supply of nutrients (Bopp et al., 2001) and Dissolved Inorganic Carbon (DIC) (Borges et al., 2008). Increasing stratification results also in a shoaling of the upper mixed layer leading to an increase in the light availability in this layer (Bopp et al., 2001).

Both ocean acidification and warming influence the distribution of DIC for calcifying organisms and therefore have the potential to alter the particulate inorganic and/or organic carbon production, which would affect the efficiency of particle export. By photosynthesis in the photic zone, phytoplankton draws down CO_2:

$$16\,CO_2 + 16\,NO_3^- + H_2\,PO_4^- + 17\,H^+ + 122\,H_2O \leftrightarrow (CH_2O)_{106}\,(NH_3)_{16}\,H_3\,PO_4 + 138\,O_2 \quad (1)$$

Published by Copernicus Publications on behalf of the European Geosciences Union.

In contrast, biogenic calcification releases CO_2:

$$Ca^{2+} + 2\,HCO_3^- \rightarrow CaCO_3 + CO_2 + H_2O \quad (2)$$

The biological carbon pump could thus remove particulate carbon from the euphotic zone by exporting it to the oceanic interior. Ballast minerals such as biogenic calcite ($CaCO_3$) enhance the flux of organic carbon from the surface ocean to the ocean floor (Armstrong et al., 2002; François et al., 2002; Klaas and Archer, 2002). The rain ratio, defined here as the ratio of Particulate Inorganic Carbon (PIC) to Particulate Organic Carbon (POC) in exported biogenic matter, determines the relative strength of the biological carbon pump and consequently the flux of CO_2 across the surface ocean-atmosphere interface.

The effect of higher pCO_2 on benthic or pelagic calcifying organisms is well documented in literature (for corals: Gattuso et al., 1998; Kleypas et al., 1999; for foraminifera: Spero et al., 1997; Bijma et al., 1999; for the coccolithophore *Emiliania huxleyi*: Riebesell et al., 2000; Zondervan et al., 2001, 2002; Sciandra et al., 2003; Delille et al., 2005; Engel et al., 2005). These studies indicated a decrease in calcification in response to an increase in CO_2. However, Langer et al. (2006) showed that this observation was not so straightforward: two species of coccolithophores, *Coccolithus pelagicus* and *Calcidiscus leptoporus*, did not exhibit the same response to increasing CO_2. Compared to cultures of *E. huxleyi*, PIC production in *C. pelagicus* cultures did not change with increasing CO_2, while *C. leptoporus* showed an optimum production of PIC under present CO_2 conditions. The authors suggested a species-specific response. In contrast to previous laboratory and field experiments involving *E. huxleyi*, Iglesias-Rodriguez et al. (2008a) showed an increase in calcification with increasing pCO_2. The response of *E. huxleyi* to increasing CO_2 levels is therefore still a matter of debate (e.g. Riebesell et al., 2008 and Iglesias-Rodriguez et al., 2008b).

Only few studies to date have tested the combined effect of increased pCO_2 and temperature on calcification, which are likely to be relevant in natural settings (for corals: Reynaud et al., 2003; for coccolithophores: Feng et al., 2008). An interacting effect of pCO_2 and temperature was found for the scleractinian coral *Stylophora pistillata*, with a 50% reduction in calcification when both parameters increased (Reynaud et al., 2003). Feng et al. (2008) demonstrated a decrease in cellular PIC content from 375 ppmV to 750 ppmV CO_2 (a decrease by 50% at 20 °C and by 41% at 24 °C) for *E. huxleyi* cultured at high light intensities (400 µmol photons $m^{-2}\,^{-1}$), but did not observe a significant effect of temperature on calcification.

In the present study, we investigated the response of the coccolithophore *E. huxleyi* grown in batch culture under different conditions of pCO_2 and temperature to assess the effect of simulated ocean acidification and warming on calcification and coccosphere size. We examined the individual and combined effects of increased pCO_2 (180 ppmV CO_2, 380 ppmV CO_2 and 750 ppmV CO_2 corresponding to past, present and future CO_2 conditions, respectively) and temperature (13 °C and 18 °C) on the POC and PIC production rates, the PIC:POC ratio, the coccosphere size spectrum, and the coccolith morphology.

2 Materials and methods

2.1 Experimental set-up and sampling

Duplicate laboratory experiments were performed on monospecific batch cultures of *E. huxleyi* (strain AC481 from Normandy, France, Algobank-Caen microalgal collection) at different pCO_2 corresponding to glacial, present and year 2100 atmospheric CO_2 concentrations by bubbling gases at fixed CO_2 concentrations (respectively 180±8 ppmV "low CO_2", 379±11 ppmV "present CO_2" and 740±16 ppmV "future CO_2" (Air Liquide, Belgium)). Experiments were carried out in 2 temperature-controlled incubators, under low, present and future CO_2 conditions at 13 °C and under present and future CO_2 conditions at 18 °C. Cells were acclimated to the experimental conditions for 10 days to avoid measuring potential adaptation effects during the dedicated experiments. The culture medium consisted of filtered (0.2 µm) and autoclaved aged surface post-bloom seawater of salinity 35.6 sampled in the northern Atlantic Ocean (47 ° 45'N, 7 ° 00'W), enriched with nitrates (NO_3) and phosphates (PO_4) to obtain final concentrations of 32 µmol L^{-1} and 1 µmol L^{-1}, respectively. Incident photon flux density was 150 µmol $m^{-2}\,s^{-1}$ and the light/dark cycle was 14 h/10 h. Cultures (8 L) were inoculated with pre-adapted cells in exponential growth phase and were grown in 10-L sized polycarbonate carboys (Nalgene). Bloom development was monitored for a period of 44 to 57 days, encompassing the exponential and the stationary growth phase. Time is referred to as d_x with x as the number of days after inoculation. Samples were taken with a sterile syringe always at the same time in the light cycle, after gentle shaking of the culturing carboys. In vivo fluorescence and turbidity (Turner fluorometer-turbidimeter) were measured daily and were used as an indicator for phytoplankton growth and calcification, respectively. Chlorophyll a (Chl-a), nutrients concentrations, cell density, POC and PIC were measured every two or three days depending on the growth phase of the culture. Additional samples for Scanning Electron Microscopy (SEM) and particle size measurement were taken as well. To allow for comparison of variables between culturing treatments we used the values corresponding to the time point after three cell generations.

2.2 Parameters of the carbonate system

The in situ pCO_2 was obtained by bubbling gases with the target CO_2 during the entire course of the experiment. Biological activity according to Eqs. (1) and (2) can modify this

in situ pCO_2. Then, pCO_2 was calculated from pH and Total Alkalinity (TA) using the CO2SYS Package (Lewis and Wallace, 1998). The dissociation constants for carbonic acid given by Mehrbach et al. (1973) as refitted by Dickson and Millero (1987) were used. pH and TA were measured every day or every two days.

TA was measured by potentiometric titration with HCl (0.1 N, Merck) using the classical Gran procedure (Gran, 1952). Data were quality checked by analysis of Certified Reference Material (A. Dickson, CDIAC). TA was corrected for nitrate and phosphate consumption according to the equation of photosynthesis of Redfield et al. (1963) (Eq. 1), using the following relation:

$$TA = TA_{measured} - \Delta\, NO_3^- - \Delta\, H_2\, PO_4^- \quad (3)$$

where ΔNO_3^- and $\Delta H_2PO_4^-$ denote the nitrate and the phosphate consumed since the beginning of the experiment (d_0) (Delille et al., 2005).

pH measurements were carried out with a combined pH electrode (Metrohm), calibrated on the Total Hydrogen Ion Concentration Scale, using TRIS (2-amino-2-hydroxymethyl-1,3-propanediol) and AMP (2-aminopyridine) buffers prepared at a salinity of 35 following Dickson (1993), and using the pK for TRIS given by Del-Valls and Dickson (1998), and that for AMP given by Dickson (1993).

2.3 Growth parameters of *E. huxleyi*

Chl-a concentration was determined following the fluorimetric method of Yentsch and Menzel (1963). Forty milliliter samples were filtered through GF/F filters under low vacuum. Filters were stored in the dark at −20 °C until analysis. For the analysis, the filters were extracted with 10 ml of 90% acetone at −20 °C overnight. Samples were then centrifuged (10 min, 4250 xg) and the fluorescence of the extract was measured with a Shimadzu RF-150 fluorometer, using an excitation wavelength of 430 nm and an emission wavelength of 663 nm. The fluorescence was calibrated with a stock solution of pure Chl-a (Merck).

Samples for nutrient measurements were filtered through Nuclepore filters (0.4 µm pore size) and filtrates were stored at −20 °C until analyses. NO_3 was determined colorimetrically with a Skalar Autoanalyzer system and PO_4 was measured manually with a spectrophotometer, both analyses followed the method of Grasshoff et al. (1983).

Cell densities were estimated by haemocytometer counting (Malassez cell) using a light microscope. Light microscopy also permitted a visual check of the health status of the culture. Growth rates (µ) were calculated as the slope of a significant linear regression of the natural logarithm of cell concentration against time over the exponential growth phase (Buitenhuis et al., 2008). Cell concentration after three generations was calculated based on the coefficients of the linear regression for each replicate culture.

POC concentration (in µmol C L^{-1}) was measured using a Fisons NA-1500 elemental analyzer. For this analysis, 40 ml of water were filtered through pre-combusted (4 h, 500 °C) GF/F filters. The measurements were carried out on the filters after the removal of carbonates by overnight exposure to strong hydrochloride acid (HCl) fumes. Calibration of the analyzer was performed using certified reference stream sediment (STSD-2) from the Geological Survey of Canada. The POC production rate during the exponential growth phase was estimated from the significant linear regression of the natural logarithm of POC concentration against time. The cellular POC production rate (P, pmol C $cell^{-1}$ d^{-1}) was determined using the following equation (Zondervan et al., 2002):

$$P = \mu \times \text{cellular carbon content} \quad (4)$$

2.4 Calcification of *E. huxleyi*

PIC concentration (in µmol C L^{-1}) was measured using a Fisons NA-1500 elemental analyzer. As for the POC analysis described above, 40 ml of water was filtered through pre-combusted (4 h, 500 °C) GF/F filters and Total Particulate Carbon (TPC) was measured on the filters. PIC was determined by subtracting the amount of POC from the amount of TPC.

TA of the seawater is also affected by calcification (or dissolution) because the precipitation of 1 mole of $CaCO_3$ reduces the TA by 2 moles (Eq. 2). $CaCO_3$ concentration (in µmol $CaCO_3$ kg SW^{-1}) could then be calculated from changes in TA using the alkalinity anomaly (Smith and Key, 1975; Chisholm and Gattuso, 1991):

$$[CaCO_3]_x = -1/2 \times (TA_x - TA_0), \quad (5)$$

where TA_x is the alkalinity on day x corrected for nutrient consumption and TA_0 is the initial alkalinity.

The measured PIC concentrations agreed well with the calculated calcite concentrations derived from changes in seawater alkalinity (Fig. 1). Because of the more frequent TA sampling during the exponential growth phase, PIC concentrations were estimated from the significant linear regression between nutrient-corrected TA and PIC concentrations, determined for each culture, increasing the reliability of the PIC production rate estimates. The cellular production rates of PIC (pmol C $cell^{-1}$ day^{-1}) were determined in analogy to the cellular POC production rates (see Eq. 4)

2.5 Coccolith morphology

For scanning electron microscopic analyses, 1 ml of sample was concentrated onto a polycarbonate Nuclepore (0.4 µm pore-size) filter. The filters were dried overnight at 50 °C, and stored dry at room temperature until analysis. The filters were fitted onto glass microscope slides with conductive glue and then sputter-coated with gold (JFC 1200, Jeolscan). Digital images of coccospheres were acquired using a Jeolscan

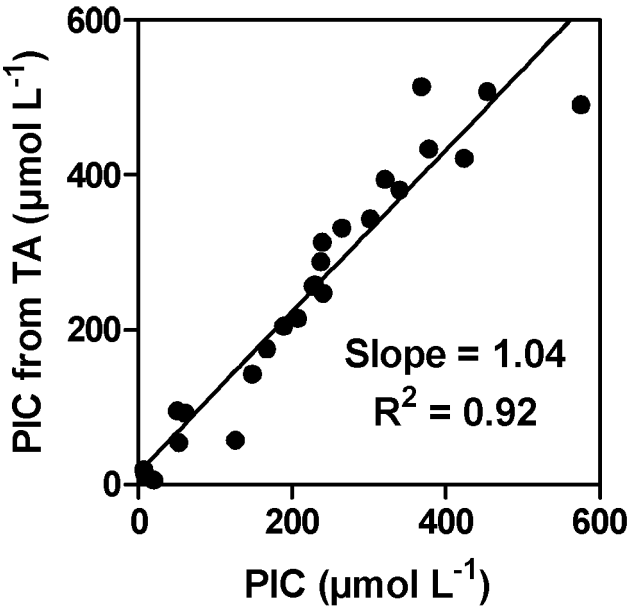

Fig. 1. Correlation between the PIC concentrations deduced from the TA measurement and those measured with a CHN analyzer. Example for the duplicate cultures at future CO_2 and 13 °C (n=25, slope = 1.042±0.064, r^2=0.92).

SEM (JSM 5600 LV) and examined at a magnification of at least 8000x.

A minimum of 100 coccoliths (attached onto the coccospheres) were analyzed per CO_2 and temperature treatment duplicate. The surface of only 1 to 2 coccoliths per coccosphere was totally exposed allowing categorization: so at least 50 coccospheres were analyzed per sample. Analyses were carried out on SEM images of *E. huxleyi* cells harvested on d_{20}, at the end of the exponential growth phase. Categorization of attached coccoliths was preferred to exclude coccoliths of unknown age and dissolution status. Coccoliths were visually classified according to four categories (Fig. 2). The first category corresponds to normal coccoliths with all segments connected and forming an oval ring. The next three categories represent stages of increasing malformation. The second one corresponds to slightly malformed coccoliths; in this category less than 5 T-segments are not well connected to others. The third category corresponds to malformed coccoliths where more than 5 T-segments are disconnected or not entirely formed. The fourth one corresponds to fragmented coccoliths; in this category parts of the coccolith are missing.

2.6 Coccosphere size frequency distribution

Size distribution of particles was determined with a Beckman Coulter Counter (Coulter Multisizer III). For each experimental treatment and for both replicates, 3 sampling time points situated around the chlorophyll maximum of the cultures were analyzed. Fixed samples (3% borate-buffered, 0.2 µm filtered, formaldehyde solution) were measured using a 50 µm aperture tube. Particle size measurements were calibrated using 10 µm latex microspheres (NIST). Particles between 2 µm and 10 µm Equivalent Spherical Diameter (ESD) were binned into 256 size classes. Only the particles between 3.5 µm and 7 µm ESD, corresponding to the *E. huxleyi* coccosphere size range, were further analyzed. On average, 5735 Coccosphere-Sized Particles (CSP) were analyzed per sample. For statistical tests, the mean particle size of CSP of each replicate was used. The volume of CSP was calculated based on that of a sphere.

2.7 Statistical treatment of data

The average value of parameters from duplicate cultures is given as the statistical mean (x) together with the minimum and maximum value (x [min;max]). Mean values were compared by means of a Student's t-test. The influence of the CO_2 treatment (13 °C) on variables was determined by means of a one-way analyse of variance (ANOVA) or a t-test. A two-way ANOVA was used to determine the statistical significance of the main effect of pCO_2 (present and future CO_2 conditions) and temperature (13 °C and 18 °C) treatments and their interaction on the variables. A Tukey post-hoc test was used to identify the source of the main effect determined by ANOVA. To assess whether the qualitative differences in coccolith morphology between temperature or pCO_2 treatments were statistically significant, either the non-parametric Mann-Whitney U test or the Kruskal-Wallis test was used, respectively. All statistical treatments of data were performed using the Statistica (7.0) software (StatSoft).

3 Results

3.1 Carbonate chemistry and bloom development in *E. huxleyi* culture experiments

The bloom development of *E. huxleyi* was followed from the beginning of the exponential growth phase. As a general feature in our culture experiments, Chl-a concentration and the particulate component increased while nutrients were consumed; a stationary phase was then reached where PO_4 became depleted and Chl-a levels slowly decreased while POC and PIC accumulated in the culture. This evolution was monitored in cultures subjected to different treatments of pCO_2 and temperature to assess the effect of ocean acidification and global warming on the organic and inorganic carbon production of *E. huxleyi*.

Parameters of the carbonate chemistry are presented in Table 1. The initial parameters correspond to values obtained on d_0, the day of inoculation of the strain. We followed the four phases of a growing culture from the lag phase to the decline and indicate also the parameters obtained at the end of the cultures. The pCO_2 was kept relatively constant during the course of the culture experiments but some variation

Table 1. Parameters of the Dissolved Inorganic Carbon (DIC) chemistry in *E. huxleyi* culture experiments corresponding to different temperature (T) and CO_2 treatment. For each parameters, the values in the first row represent the initial condition and the numbers in the second row represent the parameter at the end of the culture experiments. For pCO_2, the numbers in the third row represent the average value.

T treatment	13 °C						18 °C			
CO_2 treatment	Low CO_2		Present CO_2		Future CO_2		Present CO_2		Future CO_2	
Duplicate	1	2	1	2	1	2	1	2	1	2
pCO_2 (ppmV)	179.8	221.4	387.7	388.5	768.4	715.8	490.6	437.6	784.1	795.6
	246.9	232.2	377.8	493.9	837.9	821.2	473.8	473.2	745.3	822.8
TA (µmol kg SW^{-1})	2232.7	2230.5	2252.4	2246.0	2323.0	2326.7	2069.2	2045.0	2101.3	2152.9
	1568.3	1567.2	1652.0	1347.3	1343.1	1339.8	991.9	1090.9	1255.8	1265.4
pH	8.3	8.2	8.1	8.1	7.8	7.8	7.9	8.0	7.8	7.8
	8.1	8.1	7.9	7.8	7.6	7.6	7.7	7.6	7.6	7.5
DIC (µmol kg SW^{-1})	1817.7	1862.5	1996.1	1991.1	2177.6	2169.3	1883.1	1843.4	1982.8	2031.2
	1355.5	1345.4	1486.8	1254.4	1300.8	1296.0	935.1	887.1	1210.2	1227.4
CO_3^{2-} (µmol kg SW^{-1})	287.1	256.3	185.1	184.0	119.3	126.4	135.6	144.0	97.8	101.1
	132.7	137.6	109.5	62.1	40.2	40.7	36.5	33.0	39.1	36.5
HCO_3^- (µmol kg SW^{-1})	1524.5	1598.6	1797.7	1793.9	2032.0	2018.5	1730.8	1684.6	1858.3	1903.0
	1214.4	1199.9	1364.5	1175.5	1232.0	1227.3	882.5	838.0	1145.7	1162.9
Omega calcite	6.8	6.1	4.4	4.4	2.8	3.0	3.2	3.4	2.3	2.4
	3.2	3.3	2.6	1.5	1.0	1.0	0.9	0.8	0.9	0.9

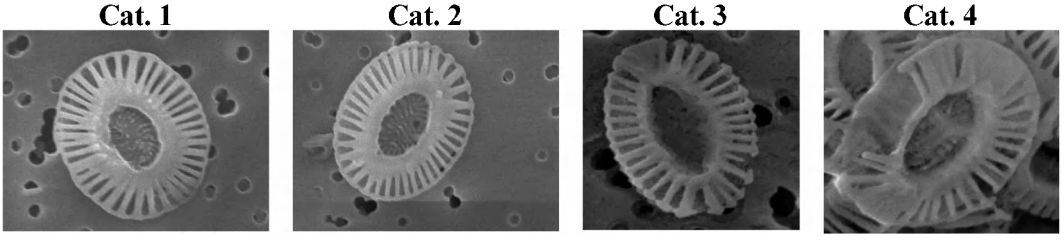

Fig. 2. Scanning electron micrographs of the four categories of coccolith morphology from normal coccoliths (cat. 1) to fragmented coccoliths (cat. 4).

occurred during the development (growth and calcification) of *E. huxleyi*. Finally, the calculated pCO_2 values in our cultures were on average always, and to some extent, higher than those of the gas bottles. Like the pCO_2, the pH varied slightly in our cultures due to biological activity. An initial increase in pH was observed in each culture during photosynthesis, followed by a decrease in pH concomitant to the occurrence of biogenic calcification. TA was constant at the beginning of the experiments and then decreased in all batch cultures, indicating calcification by *E. huxleyi*.

Maximum Chl-a concentration varied between cultures from 7.3 to 19.6 µg L^{-1} and was generally observed on around d_{20}, corresponding to PO_4 depletion. At 13 °C, a higher maximum Chl-a concentration was found in the future CO_2 cultures (17.3 [15.1; 19.6] µg L^{-1}) compared to other treatments (10.8 [9.2; 12.4] µg L^{-1} in the present CO_2/13 °C cultures and 10.3 [9.8; 10.8] µg L^{-1} in the low CO_2/13 °C cultures) (Table 2). At 18 °C, a maximum Chl-a concentration of 9.2 [8.4; 10.1] µg L^{-1} was reached in the future CO_2/18 °C treatment and 9.1 [7.3; 10.9] µg L^{-1} in the present CO_2/18 °C treatment (Table 2).

At 13 °C, maximum cell abundance was reached between d_{36} and d_{40} for future CO_2 treatments and between d_{45} and d_{52} for the experiments at present and low CO_2 (data not shown). Maximum cell densities varied from 2.22×10^5 to 3.84×10^5 cells ml^{-1} among batch cultures with highest values reached in the future CO_2 cultures (Table 2). At 18 °C, maximum cell density was reached between d_{34} and d_{40} depending on the experiment (data not shown). In the future CO_2/18 °C culture a maximum of 4.66×10^5 [4×10^5; 5.35×10^5] cells ml^{-1} was observed and 6.02×10^5 [5.2×10^5; 6.84×10^5] cells ml^{-1} in the present CO_2/18 °C treatment, (Table 2). Higher cell densities were reached in the higher temperature treatment at present CO_2 condition (two-way ANOVA, F-value$_{pCO2}$=0.4, p=0.85, and F-value$_T$=28.21, df=1, p<0.01; Tukey post-hoc, df=4, p<0.05) while no statistical difference in maximum cell abundance was observed between the future CO_2 temperature. The growth

Table 2. Summary of data, other than the DIC chemistry parameters, derived from the culture experiments.

T treatment	13 °C						18 °C			
CO_2 treatment	Low CO_2		Present CO_2		Future CO_2		Present CO_2		Future CO_2	
Duplicate	1	2	1	2	1	2	1	2	1	2
max Chl-a (μL^{-1})	9.8	10.8	9.2	12.4	19.6	15.1	8.4	10.1	10.9	7.3
max cell densities (10^5 cell ml^{-1})	2.34	2.34	2.22	2.56	3.09	2.88	6.84	5.20	5.35	4.00
Chl-a/cell (pg $cell^{-1}$)	0.22	0.12	0.07	0.08	0.14	0.12	0.05	0.05	0.03	0.03
max POC ($\mu mol\ L^{-1}$)	154.2	135.8	142.5	174.2	257.5	240.0	430.0	441.7	375.0	460.0
max PIC ($\mu mol\ L^{-1}$)	383.3	331.7	311.7	479.2	377.5	453.3	474.2	620.8	486.7	576.7
Growth rate, $\mu(d^{-1})$	0.13	0.12	0.10	0.10	0.11	0.11	0.15	0.12	0.11	0.09
pmol PIC $cell^{-1}\ d^{-1}$	0.15	0.18	0.14	0.15	0.09	0.12	0.10	0.10	0.08	0.06
pmol POC $cell^{-1}\ d^{-1}$	0.22	0.09	0.06	0.07	0.12	0.13	0.16	0.11	0.09	0.13
PIC:POC productivity ratio	0.68	2.13	2.19	2.25	0.77	0.94	0.63	0.86	0.88	0.47

rate was calculated from the increase in cell density for each treatment (Table 2). Growth rates at 13 °C were higher in the low CO_2 treatment than at higher CO_2 levels (one-way ANOVA, F-value = 20.69, df=2, $p<0.05$; Tukey post-hoc, df=3, $p<0.05$). Although growth rates for the present and future pCO_2 treatments were on average higher at higher temperature, this difference was not significant (t-value = −1.11, df=6, p=0.31).

POC increased continuously during the course of the experiments. At 13 °C, maximum POC concentration varied between 135 µmol C L^{-1} for the low CO_2 treatment and 257.5 µmol C L^{-1} for the future CO_2 treatment (Table 2). At 18 °C, maximum POC concentration ranged from 375 to 460 µmol C L^{-1} and concentrations were similar between the CO_2 treatments (Table 2). POC production was favoured by higher growth temperatures and resulted in higher POC concentrations with bloom development in the 18 °C treatments (Table 2).

3.2 Calcification in *E. huxleyi* cultures

PIC accumulated during the course of the experiments. At 13 °C, maximum PIC concentrations varied between 311.7 and 479.2 µmol C L^{-1} with maximum values obtained in the future CO_2/13 °C treatment (Table 2). At 18 °C, PIC concentrations increased from d_6 and maximum values ranged between 474.2 and 620.8 µmol L^{-1} (Table 2). In both temperature treatments, variability in PIC concentrations was observed between the CO_2 treatments and within the replicates.

3.3 Effect of pCO_2 and/or temperature on the cellular Chl-a content, POC and PIC cellular production rate and their ratio during the exponential growth phase

3.3.1 Cellular Chl-a contents

Higher cellular Chl-a contents and lower cell densities were observed at 13 °C compared to 18 °C (t-value = 3.37, df=8, $p<0.01$) (Table 2). There was no significant effect of pCO_2 at 13 °C on the cellular Chl-a content (one-way ANOVA, F-value = 2.687, df=2, p=0.214). Nonetheless, a two-way ANOVA indicated a significant effect of both temperature and pCO_2 as well as an interactive effect on the cellular Chl-a content (F-value$_{pCO2}$=9.1, F-value$_T$ = 142.3, F-value$_{pCO2*T}$ = 39.5, df=1, all $p<0.05$). The same was true when relating the cellular Chl-a content to the coccosphere volume.

3.3.2 Cellular POC production rates

POC concentration was positively correlated to *E. huxleyi* cell abundance during the cell growth phase. As a general feature, differences in the cellular POC production rates were observed among the culture experiments and among duplicate cultures (Fig. 3a).

More precisely, at 13 °C no significant trend was observed between pCO_2 treatments (one-way ANOVA, F-value = 1.30, df=2, p=0.39) (Fig. 3a). Nonetheless, cellular POC production rates were higher in the future CO_2/13 °C compared to present CO_2/13 °C treatment by 89% (t-value = 10.66, df=2, $p<0.01$).

A two-way ANOVA did not indicate a significant effect of either temperature or pCO_2 level on the cellular POC production rate at present and future CO_2 conditions (F-value$_{pCO2}$=0.74, df=1, p=0.44; F-value$_T$ = 2.26, df=1, p=0.26).

3.3.3 Cellular PIC production rates

Although a trend of decreasing cellular PIC production rates with increasing pCO_2 levels was apparent in the cultures grown at 13 °C (Fig. 3b), a one-way ANOVA did not indicate a significant effect of pCO_2 on the cellular PIC production rate (F-value = 4.51, df=2, p=0.13). The cellular PIC production rate in the treatment at 13 °C and low CO_2 level was on average 52% higher than in the future CO_2 treatment at the same temperature.

Significantly higher cellular PIC production rates were observed at lower temperature and CO_2 levels, yet no significant interaction between the two could be demonstrated (two-way ANOVA, F-value$_{pCO2}$ = 15.31, F-value$_T$ = 24.28, df=1, both $p<0.05$, and F-value$_{pCO2*T}$ = 0.19, df=1, p=0.69). The cellular PIC production rate in the treatment representing the present conditions (13 °C, 380 ppmV CO_2) were on average more than twice higher than those found under in future conditions (18 °C, 750 ppm CO_2) (Table 2 and Fig. 3b).

3.3.4 PIC:POC productivity ratio

In analogy to cellular POC production rates, no significant trend was observed for the PIC:POC productivity ratio between pCO_2 treatments at 13 °C (one-way ANOVA, F-value = 2.65, df=2, p=0.23) (Fig. 3c).

Significantly higher PIC:POC productivity ratio's were observed at lower temperature and pCO_2 levels, and a significant interactive effect between the two could be demonstrated (two-way ANOVA, F-value$_{pCO2}$ = 33.26, F-value$_T$ = 44.45, and F-value$_{pCO2*T}$ = 27.14, df=1, all $p<0.01$). A Tukey post-hoc test indicated that this was mainly due to the significantly higher PIC:POC ratio's encountered in the treatment representing present conditions (13 °C, 380 ppm CO_2) compared to the treatments under the future conditions (df=4, all $p<0.01$).

With an increase in temperature, the ratio decreased on average by almost a factor 3 in the present CO_2 treatment but remained equal in the future CO_2 treatment.

3.4 Coccolith morphology

SEM analysis revealed variable degrees of coccolith malformation (Fig. 4). A significant effect of the CO_2 treatments on coccolith morphology was found at 13 °C (Kruskal-Wallis test, H(2, 616)=68.10, $p<0.0001$) as well as at 18 °C (Mann-Whitney U test, Z-value = −6.52, $p<0.0001$) while temperature did not significantly affect coccolith morphology (Mann-Whitney U test, Z-value$_{present}$ = 0.83, $p_{present}$ = 0.41, and Z-value$_{future}$ = −1.31, p_{future} = 0.19). The percentage of normal coccoliths was more important in the cultures under low CO_2/13 °C conditions (43%) than under present CO_2 condition with 22% in the 13 °C and 29% in the 18 °C treatment. Finally, the lowest percentage of normally formed coccoliths was observed in the future CO_2 treatments, with 13% and 9% at 13 °C and 18 °C, respectively. The percentage of malformed coccoliths increased with increasing pCO_2, with 23% and 28% of fragmented coccoliths observed in the future CO_2 treatment at 13 °C and 18 °C, respectively, while only 7% of the coccoliths were fragmented in the low CO_2/13 °C experiment.

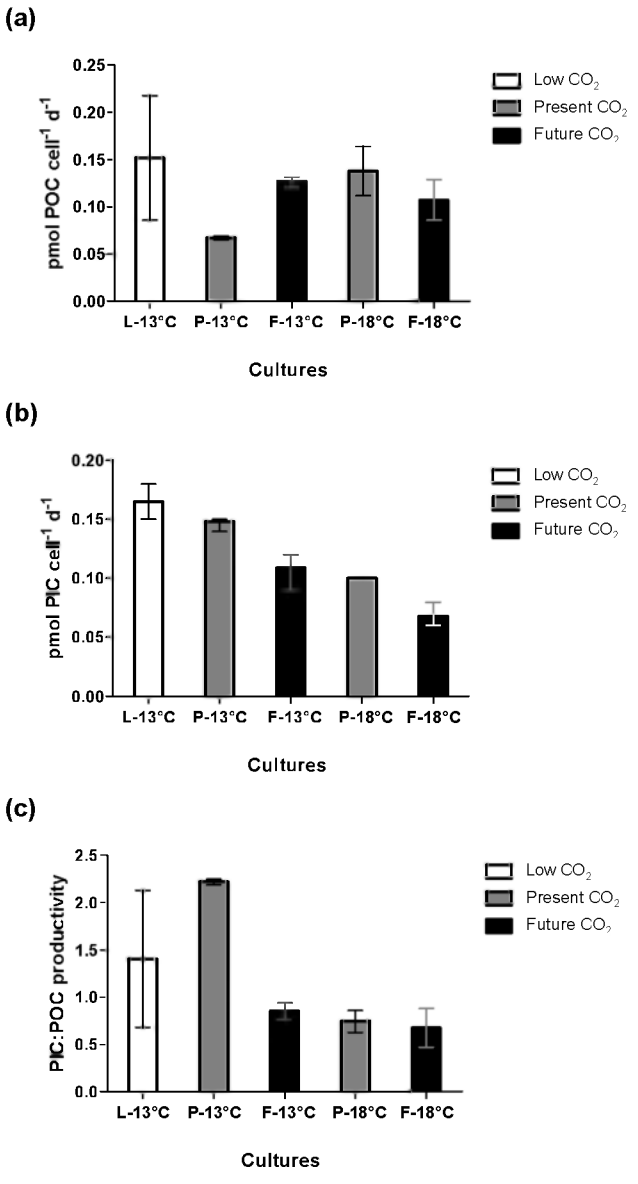

Fig. 3. **(a)** Cellular POC production rate, **(b)** cellular PIC production rate and **(c)** PIC:POC productivity ratio during the exponential phase of the batch culture experiments. Bars represent the mean of the duplicate cultures and the whiskers represent the minimum and maximum measurements.

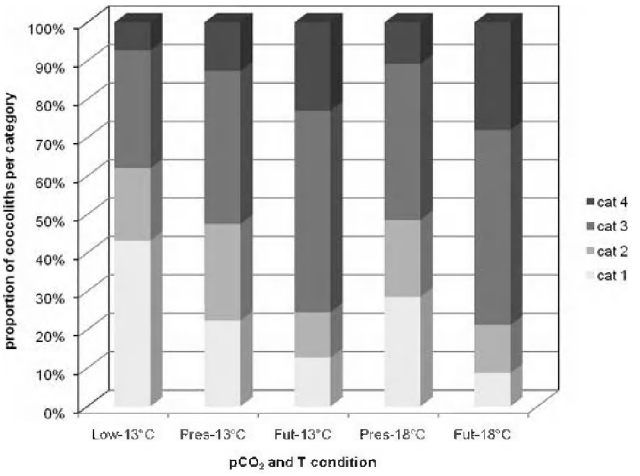

Fig. 4. Percentage of coccoliths per category, from normal coccoliths (cat. 1) to fragmented coccoliths (cat. 4), for each treatment of pCO_2 and temperature.

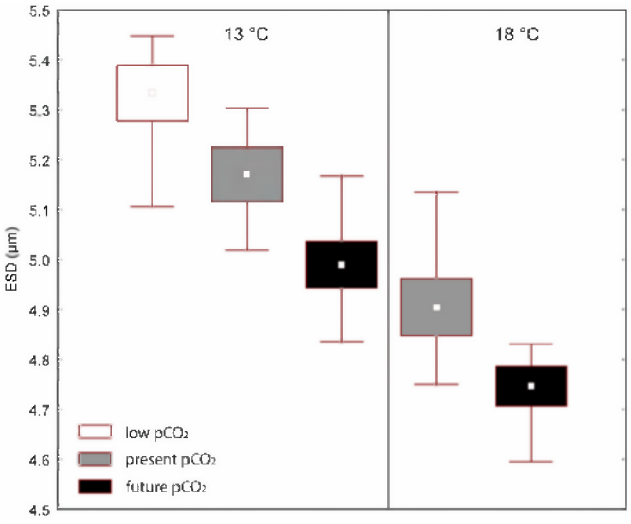

Fig. 5. Mean particle size of CSP for each treatment. The central marker denotes the mean, the standard error is given by the box boundaries, and the whiskers represent the minimum and maximum mean values of the size measurement on three time points in duplicate cultures (n=6). The white box represents the low CO_2 treatment, the grey shaded boxes the present CO_2 treatments, and the black boxes the future CO_2 treatments. The right-most two boxes represent the 18 °C treatments.

3.5 Coccosphere size frequency distribution

The mean particle size of CSP was significantly different between the different CO_2 and temperature treatments (ANOVA, F-value = 11.27, df=4, $p<0.01$) (Fig. 5). A clear trend in CSP ESD reduction was observed with increasing pCO_2 and temperature treatments. Smaller CSP were found in the cultures grown at higher CO_2 levels and at 13 °C ($ANOVA_{13°C}$, F-value = 10.63, df=2, $p<0.001$), with CSP smaller in the future CO_2 than in the low CO_2 treatment (Tukey post-hoc test, df=15, $p<0.01$) (Fig. 5). Both temperature as well as seawater CO_2 concentration had a significantly negative effect on the mean particle size of CSP (two-way ANOVA, F-$value_{pCO2}$ = 11.35, F-$value_T$ = 25.60, all df=1 and $p<0.01$), yet temperature did not significantly exacerbate the effect of CO_2 on the mean CSP size (two-way ANOVA, F-$value_{pCO2*T}$ = 0.05, p=0.83). A Tukey post-hoc test indicated that the source of the main effects originated from the significant differences in CSP size between the present pCO_2/13 °C treatment and the treatments at 18 °C (present and future), and between the 13 °C and 18 °C treatments at future pCO_2 (df=20, all $p<0.01$).

4 Discussion

4.1 Impact of increasing CO_2 and temperature on the growth rate

Contrary to the observations made in previous studies (Montagnes and Franklin, 2001; Atkinson et al., 2003), in our experiments growth rates did not show in general a clear positive trend with increasing temperature. Growth rates observed during this study were slower than those commonly observed for *E. huxleyi* in batch cultures that ranged generally between 0.2 and 1.4 d^{-1} depending on growth conditions such as temperature, light or CO_2 levels (Zondervan et al., 2002; Buitenhuis et al., 2008; Iglesias-Rodriguez et al., 2008). Macronutrient enrichments used in previous studies are often higher than those in our investigation. Culture media such as f/2 (Guillard, 1975; Guillard and Ryther, 1962) or K/5 (Keller et al., 1985) enriched with trace metals and vitamins are generally utilized. It is possible that the omission of trace element (iron, zinc or cobalt) and/or the lack of vitamins as well as the lower macronutrient enrichment all contributed to the slower growth of our batch cultures. This is supported by measurements made on cultures (of the same *E. huxleyi* strain) that were conducted in our laboratory with and without the addition of trace metals and vitamins (V. Carbonnel, personal communication, 2009). Comparison of the growth rate between our culture experiments is warranted, since they all benefitted from the same nutrient enrichment.

4.2 Impact of increasing CO_2 and temperature on the POC production

An increase in cellular POC production rate was found in the future CO_2 compared to the present CO_2 treatment (at 13 °C). In our experiments, no clear effect of the pCO_2 on the cellular POC production rate was observed, as was sometimes the case in previous studies that showed contradictory results. In batch culture experiments, an increase in the POC production (Riebesell et al., 2000; Zondervan et al., 2001)

is generally observed with increasing CO_2 levels while in mesocosm experiments no significant changes were observed (Delille et al., 2005). However, a higher loss of POC in the future CO_2 mesocosm was due to organic matter export.

In some treatments corresponding to future conditions (future CO_2/13 °C, present CO_2/18 °C, future CO_2/18 °C), higher POC concentrations than expected from the Redfield stoichiometry were nonetheless measured. This suggests the occurrence of carbon overconsumption, which refers to a continuous uptake of DIC by phytoplankton after nutrient exhaustion (Banse, 1994). Indeed, the consumption of 32 µmol L^{-1} of nitrate would yield a theoretical 212 µmol L^{-1} of POC. The DIC consumed by the algal cell after nutrient exhaustion cannot be further metabolised into cell constituents, such as proteins or nucleic acids, due to the limitation of nutrients (N and P) and is therefore released as dissolved or colloidal carbon-rich organic material, such as polysaccharides that aggregate to complement the POC pool.

4.3 Impact of increasing CO_2 and temperature on the PIC production

The cellular PIC production rates decreased with increasing pCO_2 and temperature, as illustrated by a reduction by 52% between the low and the future CO_2 treatment at 13 °C. While the different pCO_2 conditions were simulated by bubbling gases at fixed CO_2 concentrations, we obtained results similar to Riebesell et al. (2000) and Zondervan et al. (2001) who modified the pCO_2 by the addition of acid/base instead. The effect of increasing pCO_2 on *E. huxleyi* is rather well studied and it is generally accepted that calcification decreases with increasing pCO_2, although the study of Iglesias-Rodriguez et al. (2008a) showed contradicting results. Langer et al. (2009) attributed the different responses observed by the fact that different strains were used during the various studies. These authors showed that 4 strains of *E. huxleyi* responded differently to different CO_2 levels and proposed that the strain specific response has genetic bases (cfr. strain selection as in Lakeman et al., 2009).

Rost et al. (2008) encouraged studies manipulating multiple environmental factors to assess their interactive effects. In addition to the pCO_2, we also investigated the effect of temperature on bloom variables. The cellular calcification rate decreased from the low CO_2/13 °C to the future CO_2/18 °C treatment by 59%, yet no significant interacting effect of pCO_2 and temperature on calcification was found. Increasing the temperature by 5 °C decreased the cellular calcification rate by 49% in the culture at present CO_2 and by 60% in the one at future CO_2.The latter result was not corroborated by Feng et al. (2008) who also studied the interactive effect of pCO_2 (375 ppmV and 750 ppmV) and temperature (20 and 24 °C) at two different irradiances (50 and 400 µmol m^{-2} s^{-1}) using semi-continuous laboratory cultures. As in our study, these authors observed a reduction in the biomass-normalized PIC production rate with increasing pCO_2, but only at high irradiance (400 µmol m^{-2} s^{-1}). The decrease in cellular calcite production rates at high pCO_2 could be explained by: (1) a lower calcite content per coccolith (2) a decrease in coccolith number per coccolithophore cell or (3) a decrease in coccolith production rate, all of them not mutually exclusive. Our data suggest, however, a reduction in the number of coccoliths per cell as evidenced by the smaller coccospheres observed under future CO_2 conditions. In addition, SEM examinations of coccolith morphology point towards a lower calcite content per coccolith at high pCO_2.

4.4 Impact of increasing CO_2 and temperature on the coccosphere size

The growth rate showed a positive trend with temperature (at 380 ppm and 750 ppm) while a decrease in coccosphere size in parallel to a decrease in calcification was observed. Sorrosa et al. (2005) also found that a higher growth temperature would induce a reduction in cell size and intracellular calcification in *E. huxleyi*.

A reduction in the mean coccosphere volume by 10% (±1%) was observed across treatments with increasing pCO_2. This result is in accordance with Engel et al. (2005) who found a smaller coccosphere size at high CO_2 concentrations. The observed decrease of the mean size of CSP with increasing temperature and CO_2 conditions either suggests a biovolume reduction or a decrease in coccolith cell coverage. Coulter size determinations are based on the measurement of the electrical signal generated by displacement of an electrolyte volume and thus no differentiation can be made between the share of biovolume and coccoliths making up the coccosphere. Biovolume measurements to determine the cellular organic carbon content could therefore be performed in further studies by microscopic staining of the cytosol or by dissolving the coccoliths prior to size analysis by the Coulter method (Buitenhuis et al., 2008).

Cell volume in protists is known to decrease while cell division rate increases with increasing temperature (Montagnes and Franklin, 2001; Atkinson et al., 2003). Here, we noted a decrease in coccosphere volume of 3% per °C (present and future CO_2 treatments), which is in accordance with the values for biovolume reduction proposed by Atkinson et al. (2003).

4.5 Impact of increasing CO_2 and temperature on the coccolith morphology

The cellular calcification rate (expressed in pmol PIC $cell^{-1}$ d^{-1}) decreased while the percentage of aberrant coccoliths increased, suggesting that the decrease in PIC $cell^{-1}$ was due to altered calcite content per coccoliths (Fig. 6). Changes in PIC production have already been associated with alterations of coccolith morphology (Langer et al., 2006). Riebesell et al. (2000) have also documented

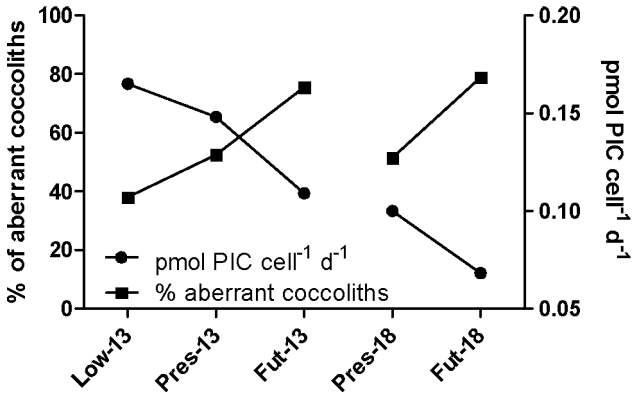

Fig. 6. Percentage of aberrant coccoliths (sum of the category 3 and 4) (solid squares) and cellular PIC production rate (solid circles) per CO_2/temperature treatments.

E. huxleyi cells with malformed coccoliths or an incomplete coccosphere in high pCO_2 cultures. Contrary to our results, Iglesias-Rodriguez et al. (2008a) observed an increase in the PIC production with increasing pCO_2 associated with an increase in the coccolith size. While no effect of temperature on coccolith morphology could be detected in our study, Watabe and Wilbur (1966) found that the percentage of abnormal coccolith increased at lower and higher temperature extremes (cultures at 7, 12, 18, 24 and 27 °C). Our temperature range may be too small to observe such an effect.

5 Conclusions

In the light of our experimental results, *E. huxleyi* is sensitive to changes in pCO_2 and temperature. Coccosphere-sized particles showed a size reduction trend with both increasing temperature and pCO_2. The cellular calcite production rate was shown to be lower under future CO_2 and temperature conditions. This could lead to a smaller ballast effect and thus a reduction in C export as highlighted by lower PIC:POC ratios measured in the future treatments of our culture experiments.

A lower cellular calcite content can thus be expected under future pCO_2 conditions, which is reflected by the deteriorated coccolith morphology determined in our study, while no significant effect of temperature on the coccolith morphology was observed. The sole future increase in pCO_2 may thus have a greater adverse impact on the calcification of *E. huxleyi* than the increase in temperature alone or the interacting effects of temperature and pCO_2.

Acknowledgements. Nathalie Roevros is gratefully acknowledged for her technical assistance in the laboratory. We would like to thank A. Borges, B. Delille and K. Suykens from the University of Liège for their assistance in the measurements of pH and DIC and for their fruitful comments. The comments of the two anonymous reviewers are greatly acknowledged, which improved the clarity of this paper. C. De Bodt was supported by a PhD grant from the EU FP6 IP CarboOcean project (contract no. 511176–2). N. Van Oostende received a PhD grant from the Institute for the Promotion of Innovation through Science and Technology in Flanders (IWT-Vlaanderen). This study was also funded by Belgian Federal Science Policy Office in the framework of the PEACE project (contract numbers SD/CS/03A and SD/CS/03B). It is also a contribution to the EU FP7 IP EPOCA project (contract no. 211384). The present work is a Belgian contribution to the international SOLAS project.

Edited by: A. Shemesh

References

Armstrong, R. A., Lee, C., Hedges, J. I., Honjo, S., and Wakeham, S. G.: A new, mechanistic model for organic carbon fluxes in the ocean based on the quantitative association of POC with ballast minerals, Deep-Sea Res., 49, 219–236, 2002.

Atkinson, D. A., Ciotti, B. J., and Montagnes, D. J. S.: Protists decrease in size linearly with temperature: ca. 2.5% °C^{-1}, Philos. T. Roy. Soc. B, 270, 2605–2611, 2003.

Banse, K.: Uptake of inorganic carbon and nitrate by marine plankton and the Redfield ratio, Global Biogeochem. Cy., 8, 81–84, 1994.

Bijma, J., Spero, H. J., and Lea, D. W.: Reassessing Foraminiferal Stable Isotope Geochemistry: Impact of the Oceanic Carbonate System (Experimental Results), in: Use of Proxies in Paleoceanography: Examples from the South Atlantic, edited by: Fischer, G. and Wefer, G., Springer-Verlag, Berlin Heidelberg, 489–512, 1999.

Bopp, L., Monfray, P., Aumont, O., Dufresne, J.-L., Le Treut, H., Madec, G., Terray, L., and Orr, J. C.: Potential impact of climate change on marine export production, Global Biogeochem. Cy., 15, 81–99, 2001.

Borges, A. V., Tilbrook, B., Metzl, N., Lenton, A., and Delille, B.: Inter-annual variability of the carbon dioxide oceanic sink south of Tasmania, Biogeosciences, 5, 141–155, 2008, http://www.biogeosciences.net/5/141/2008/.

Buitenhuis, E. T., Pangerc, T., Franklin, D. J., Le Quéré, C., and Malin, G.: Growth rates of six coccolithophorid strains as a function of temperature, Limnol. Oceanogr., 53, 1181–1185, 2008.

Canadell, J. G., Le Quéré, C., Raupach, M. R., Field, C. B., Buitenuis, E. T., Ciais, P., Conway, T. J., Gillett, N. P., Houghton, R. A., and Marland, G.: Contributions to accelerating atmospheric CO_2 growth from economic activity, carbon intensity, and efficiency of natural sinks, P. Natl. Acad. Sci. USA, 104, 18866–18870, 2007.

Chisholm, J. R. M. and Gattuso, J.-P.: Validation of the alkalinity anomaly technique for investigating calcification and photosynthesis in coral reef communities, Limnol. Oceanogr., 36, 1232–1239, 1991.

Delille, B., Harlay, J., Zondervan, I., Jacquet, S., Chou, L., Wollast, R., Bellerby, R. G. J., Frankignoulle, M., Borges, A. V., Riebesell, U., and Gattuso, J.-P.: Response of primary production and calcification to changes of pCO_2 during experimental blooms of the coccolithophorid *Emiliania huxleyi*, Global Biogeochem. Cy., 19, GB2023, doi:10.1029/2004GB002318, 2005.

DelValls, T. A. and Dickson, A. G.: The pH of buffers based on 2-amino-2-hydroxymethyl-1,3-propanediol ("tris") in synthetic sea water, Deep-Sea Res. Pt. I, 45, 1541–1554, 1998.

Dickson, A. G.: The measurement of seawater pH, Mar. Chem., 44, 131–142, 1993.

Dickson, A. G. and Millero, F. J.: A comparison of the equilibrium constants for the dissociation of carbonic acid in seawater media, Deep-Sea Res. Pt. I, 34, 1733–1743, 1987.

Engel, A., Zondervan, I., Aerts, K., Beaufort, L., Benthien, A., Chou, L., Delille, B., Gattuso, J.-P., Harlay, J., Heemann, C., Hoffmann, L., Jacquet, S., Nejstgaard, J., Pizay, M.-D., Rochelle-Newall, E., Schneider, U., Terbrueggen, A., and Riebesell, U.: Testing the direct effect of CO_2 concentration on a bloom of the coccolithophorid *Emiliania huxleyi* in mesocosm experiments, Limnol. Oceanogr., 50, 493–507, 2005.

Feng, Y., Warner, M. E., Zhang, Y., Sun, J., Fu, F.-X., Rose, J. M., and Hutchins, D. A.: Interactive effects of increased pCO_2, temperature and irradiance on the marine coccolithophore *Emiliania huxleyi* (Prymnesiophyceae), Eur. J. Phycol., 43, 87–98, 2008.

François, R., Honjo, S., Krishfield, R. A., and Manganini, S. J.: Factors controlling the flux of organic carbon to the bathypelagic zone of the ocean, Global Biogeochem. Cy., 16, 1–19, 2002.

Gattuso, J.-P., Frankignoulle, M., Bourge, I., Romaine, S., and Buddemeier, R. W.: Effect of calcium carbonate saturation of seawater on coral calcification, Global Planet. Change, 18, 37–46, 1998.

Gran, G.: Determination of the equivalence point in potentiometric titrations, Part II, Analyst, 77, 661–671, 1952.

Grasshoff, K., Ehrhardt, M., and Kremling, K.: Methods of Seawater Analysis, Verlag Chemie, Weinheim, 2nd edition, 419 pp., 1983.

Guillard, R. R. L.: Culture of phytoplankton for feeding marine invertebrates, in: Culture of Marine Invertebrate Animals, edited by: Smith, W. L. and Chanley, M. H., Plenum Press, New York, USA, 26–60, 1975.

Guillard, R. R. L. and Ryther, J. H.: Studies of marine planktonic diatoms, I. Cyclotella nana Hustedt and Detonula confervacea Cleve, Can. J. Microbiol., 8, 229–239, 1962.

Iglesias-Rodriguez, M. D., Halloran, P. R., Rickaby, R. E. M., Hall, I. R., Colmenero-Hidalgo, E., Gittins, J. R., Green, D. R. H., Tyrrel, T., Gibbs, S. W., von Dassow, P., Rehm, E., Armbrust, E. V., and Boessenkool, K. P.: Phytoplankton calcification in a high-CO_2 world, Science, 320, 336–340, 2008a.

Iglesias-Rodriguez, M. D., Buitenhuis, E. T., Raven, J. A., Schofield, O., Poulton, A. J., Gibbs, S., Halloran, P. R., and de Baar, H. J. W.: Response to comment on "Phytoplankton calcification in a high-CO_2 world", Science, 322, 1466c, doi:10.1126/Science.1161501, 2008b.

IPCC: Climate Change 2007: Synthesis Report, Contribution of Working Groups I, II and III to the Fourth Assessment Report of the Intergovernmental Panel on Climate Change, edited by: Core Writing Team, Pachauri, R. K., and Reisinger, A., IPCC, Geneva, Switzerland, 104 pp., 2007.

Keller, M. D., Selvin, R. C., Claus, W., and Guillard, R. R. L.: Media for the culture of oceanic ultraphytoplankton, J. Phycol., 23, 633–638, 1987.

Klaas, C. and Archer, D. E.: Association of sinking organic matter with various types of mineral ballast in the deep sea: Implications for the rain ratio, Global Biogeochem. Cy., 16, 63-1–63-14, 2002.

Kleypas, J., Buddemeier, R. W., Archer, D., Gattuso, J.-P., Langdon, C., and Opdyke, B. N.: Geochemical consequences of increased atmospheric carbon dioxide on corals reefs, Science, 284, 118–120, 1999.

Lakeman, M. B., von Dassow, P., and Cattolico, R. A.: The strain concept in phytoplankton ecology, Harmful Algae, 8(5), 746–758, 2009.

Langer, G., Geisen, M., Baumann, K.-H., Kläs, J., Riebesell, U., Thoms, S., and Young, J. R.: Species-specific responses of calcifying algae to changing seawater chemistry, Geochem. Geophy. Geosy., 7, 1–12, 2006.

Langer, G., Nehrke, G., Probert, I., Ly, J., and Ziveri, P.: Strain-specific responses of *Emiliania huxleyi* to changing seawater carbonate chemistry, Biogeosciences, 6, 2637–2646, 2009, http://www.biogeosciences.net/6/2637/2009/.

Lewis, E. and Wallace, D. W. R.: CO_2SYS Program developed for CO_2 system calculations, ORNL/CDIAC-105, Carbon Dioxide Information Analysis Center, Oak Ridge National Laboratory, US Department of Energy, Oak Ridge, Tennessee, 1998.

Mehrbach, C., Culberson, C. H., Hawley, J. E., and Pytkowicz, R. N.: Measurement of the apparent dissociation constants of carbonic acid in seawater at atmospheric pressure, Limnol. Oceanogr., 18, 897–907, 1973.

Montagnes, D. J. S. and Franklin, D. J.: Effect of temperature on diatom volume, growth rate, and carbon and nitrogen content: Reconsidering some paradigms, Limnol. Oceanogr., 46, 2008–2018, 2001.

Redfield, A. C., Ketchum, B. M., and Richards, F. A.: The influence of organism on the composition of seawater, in: The sea, edited by: Hill, N. M., 2nd edn., Wiley, 26–77, 1963.

Reynaud, S., Leclercq, N., Romaine-Lioud, S., Ferrier-Pagès, C., Jaubert, J., and Gattuso, J.-P.: Interacting effect of CO_2 partial pressure and temperature on photosynthesis and calcification in a scleractinian coral, Global Change Biol., 9, 1660–1668, 2003.

Riebesell, U., Zondervan, I., Rost, B., Tortell, P. D., Zeebe, R. E., and Morel, F. M. M.: Reduced calcification of marine plankton in response to increased atmospheric CO_2, Nature, 407, 364–367, 2000.

Riebesell, U., Bellerby, R., Engel, A., Fabry, V. J., Hutchins, D. A., Reusch, T. B. H., Schulz, K. G., and Morel, F. M. M.: Comment on "Phytoplankton calcification in a high-CO_2 world", Science, 322, 1466b, doi:10.1126/Science.1161096, 2008.

Rost, B., Zondervan, I., and Wolf-Gladrow, D.: Sensitivity of phytoplankton to future changes in ocean carbonate chemistry: current knowledge, contradictions and research directions, Mar. Ecol.-Prog. Ser., 373, 227–237, 2008.

Sciandra, A., Harlay, J., Lefèbvre, D., Lemée, R., Rimmelin, P., Denis, M., and Gattuso, J.-P.: Response of coccolithophorid *Emiliania huxleyi* to elevated partial pressure of CO_2 under nitrogen limitation, Mar. Ecol.-Prog. Ser., 261, 111–122, 2003.

Smith, S. V. and Key, G. S.: Carbon dioxide and metabolism in marine environments, Limnol. Oceanogr., 20, 493–495, 1975.

Sorrosa, J. M., Satoh, M., and Shiraiwa, Y.: Low temperature stimulates cell enlargement and intracellular calcification of coccolithophorids, Mar. Biotechnol., 7, 128–133, 2005.

Spero, H. J., Bijma, J., Lea, D. W., and Bernis, B. E.: Effect of seawater carbonate concentration on foraminiferal carbon and oxygen isotopes, Nature, 390, 497–500, 1997.

Watabe, N. and Wilbur, K. M.: Effects of temperature on growth, calcification, and coccolith form in *Coccolithus huxleyi* (Coccolithineae), Limnol. Oceanogr., 11, 567–575, 1966.

Yentsch, C. S. and Menzel, D. W.: A method for the determination of phytoplankton chlorophyll and phaeophytin by fluorescence, Deep-Sea Res., 10, 221–231, 1963.

Zeebe, R. E. and Wolf-Gladrow, D.: CO_2 in seawater: equilibrium, kinetics, isotopes, Elsevier Oceanography Series, Elsevier, Amsterdam, 346 pp., 2001.

Zondervan, I., Zeebe, R. E., Rost, B., and Riebesell, U.: Decreasing marine biogenic calcification: A negative feedback on rising atmospheric pCO_2, Global Biogeochem. Cy., 15, 507–516, 2001.

Zondervan, I., Rost, B., and Riebesell, U.: Effect of CO_2 concentration on the PIC/POC ratio in the coccolithophore *Emiliania huxleyi* grown under light-limiting conditions and different daylengths, J. Exp. Mar. Biol. Ecol., 272, 55–70, 2002.